FIRE: a near-infrared, cross-dispersed echellette spectrometer for the Magellan telescopes

Robert A. Simcoe[a], Adam J. Burgasser[a], Rebecca A. Bernstein[b], Bruce C. Bigelow[b], Jason Fishner[a], William J. Forrest[c], Craig McMurtry[c], Judith L. Pipher[c], Paul L. Schechter[a], Matthew Smith[a],

[a]MIT-Kavli Center for Astrophysics and Space Research, Cambridge, MA USA 02139;
[b]UCO/Lick Observatory, Santa Cruz, CA USA 95064;
[c]Dept of Physics and Astronomy, University of Rochester, Rochester, NY USA 14627

ABSTRACT

FIRE (the Folded-port InfraRed Echellette) is a prism cross-dispersed infrared spectrometer, designed to deliver single-object R=6000 spectra over the 0.8-2.5 micron range, simultaneously. It will be installed at one of the auxiliary Nasmyth foci of the Magellan 6.5-meter telescopes. FIRE employs a network of ZnSe and Infrasil prisms, coupled with an R1 reflection grating, to image 21 diffraction orders onto a 2048 x 2048, HAWAII-2RG focal plane array. Optionally, a user-controlled turret may be rotated to replace the reflection grating with a mirror, resulting in a single-order, longslit spectrum with R ~ 1000. A separate, cold infrared sensor will be used for object acquisition and guiding. Both detectors will be controlled by cryogenically mounted SIDECAR ASICs. The availability of low-noise detectors motivates our choice of spectral resolution, which was expressly optimized for Magellan by balancing the scientific demand for increased R with practical limits on exposure times (taking into account statistics on seeing conditions). This contribution describes that analysis, as well as FIRE's optical and opto-mechanical design, and the design and implementation of cryogenic mechanisms. Finally, we will discuss our data-flow model, and outline strategies we are putting in place to facilitate data reduction and analysis.

Keywords: Infrared, spectrograph, echelle

1. SCIENCE GOALS AND DESIGN MOTIVATION

Recent advances in the study of high-redshift galaxy assembly, QSO formation, star formation at low mass and in obscured environments, planetary astronomy, and gamma-ray bursts have all highlighted the utility of medium-resolution, low background infrared spectroscopy. There exists a strong heritage of near-infrared spectrometers designed for either low-resolution (R < 3000) observation of faint sources, or high-resolution (R > 10,000) observation of bright sources. Today, improvements in both the format and dark current of HgCdTe detectors have enabled the design of moderate resolution spectrometers that can target intrinsically faint astronomical objects. We are constructing a new infrared spectrometer named FIRE (the Folded port InfraRed Echellette) for the 6.5m Magellan telescopes with this parameter space in mind.

A particular scientific goal for FIRE is the study of high redshift QSO absorption lines, which present particular challenges from the ground at infrared wavelengths. The faint magnitudes of high redshift targets, contrasted with the realities of bright foregrounds, drive the choice of spectral resolution in opposite directions. An ideal instrument must deliver high sensitivity with low instrumental background (for faint targets), moderate-to-high spectral resolution (to resolve weak, intrinsically narrow lines), avoidance of hydroxyl sky emission (which eliminates redshift path) and complete wavelength coverage from 0.8-2.5 microns (since the redshifts of absorbers are unknown *a priori,* and to overlap with optical instruments at the blue end).

To aid in the choice of FIRE's resolution, we constructed a simple model of a spectrograph coupled to a 6.5 meter telescope with Magellan's seeing performance, and considered the tradeoff between OH avoidance (which drives toward high resolution) and signal-to-noise ratio (SNR, which drives toward low resolution). We modeled the OH sky emission spectrum after Martini & Depoy[1] and Rousselot et al[2], estimating the fraction *f* of spectral pixels free of OH

Ground-based and Airborne Instrumentation for Astronomy II, edited by Ian S. McLean, Mark M. Casali,
Proc. of SPIE Vol. 7014, 70140U, (2008) · 0277-786X/08/$18 · doi: 10.1117/12.790414

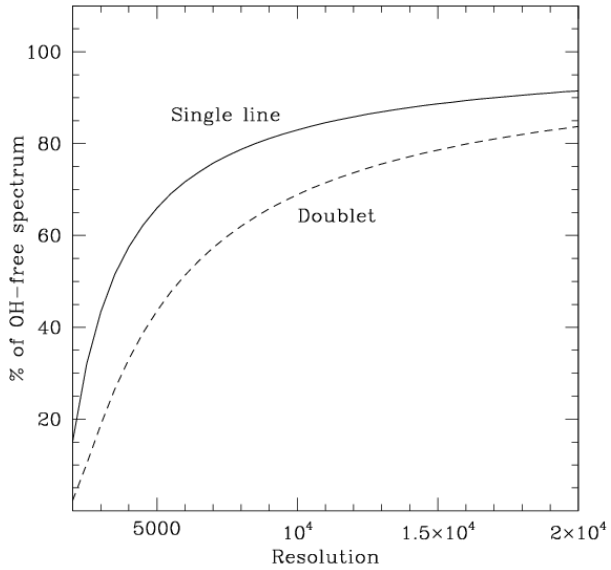

Figure 1: Fraction of spectral pixels free of OH contamination, as a function of spectral resolution

contamination as a function of spectral resolution. For observations of a single line, this is a good figure of merit for "clean" spectrum, but for doublets (such as C IV) the relevant figure is f^2, and triples (O III/Hα/Hβ) it is f^3. Figure 1 illustrates these effects for single lines and doublets. There is a clear increase in observable pathlength with increasing spectral resolution ($R = \lambda/\Delta\lambda$) up to R ~ 10,000, after which the sky emission is effectively suppressed and the curves level out. However, at the highest resolutions, individual objects with J ~ 18-20 (characteristic of high redshift quasars or the faintest brown dwarfs) would require exposure times that are many hours long. Our noise model focused on sources in this range, using appropriate parameters for modern HgCdTe detectors and instrument and sky backgrounds. For inter-line sky brightness, we used several estimates ranging from Maihara's[3] measurements at Mauna Kea to the Gemini integration time calculator's estimate (which is roughly a factor of two higher). There is substantial evidence that this inter-line background is higher than the "true" interline continuum[4], but we felt that these numbers adequately represented the background in realistic instruments, including scattered light effects. We calculated the number of hours required to reach SNR = 10 for sources at 19th magnitude, and defined our figure of merit as the fraction of OH-free spectrum divided by this exposure time.

We found a broad maximum in the merit function centered on R = 6000, or 50 km/s for combinations of 1, 2, or 3 lines, and have chosen this value for FIRE's baseline resolution. This is an astrophysically interesting velocity scale, and it is well matched to optical echellettes such as MagE on Magellan and ESI[5] on Keck. It is sufficiently fine to pass the "elbow" in the OH curve shown in Figure 1, yet coarse enough to permit integration times of one to a few hours on Magellan for faint targets. Of course, the exact location of this optimum is particular to Magellan, so the analysis is not generic and would need to be customized for use with other telescopes and sites.

Once FIRE's spectral resolution was set, our choice of slit size was motivated by site conditions at Magellan, and the requirement that a "typical" slit deliver R=6000. Figure 2 shows a histogram of the J-band seeing compiled during four years of science observations on the Magellan Baade telescope. From this, we selected 0.6 arcseconds as FIRE's nominal slit width, since this encompasses all but the high-end tail of the seeing distribution. To accommodate the best seeing conditions, we selected a pixel pitch of 0.18 arcseconds in the spectral direction, corresponding to a 2-pixel slit of 0.36 arcseconds at R=10,000 (30 km/s).

2. OPTICAL DESIGN

FIRE's optical configuration has been kept as simple as possible with primary goals of achieving high throughput, observing flexibility, and a minimal number of cryogenic mechanisms. To this end, we use a multi-prism and fixed-angle grating configuration to obtain full spectral coverage from 0.82 to 2.51 μm. A combination of ZnSe and Infrasil prisms provide relatively uniform order spacing over a factor of three in wavelength, at higher throughput than a grating would allow (because of its blaze function).

The instrument contains four main optical subassemblies: an Offner[6] relay, a collimator, dispersing elements, and a camera.

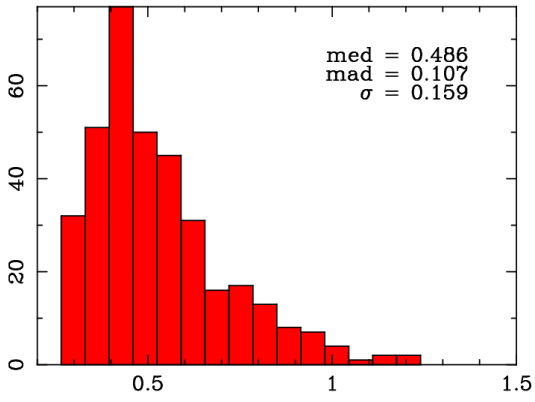

Figure 2: J band natural seeing statistics at Magellan over a four-year observing period (courtesy C. Burns)

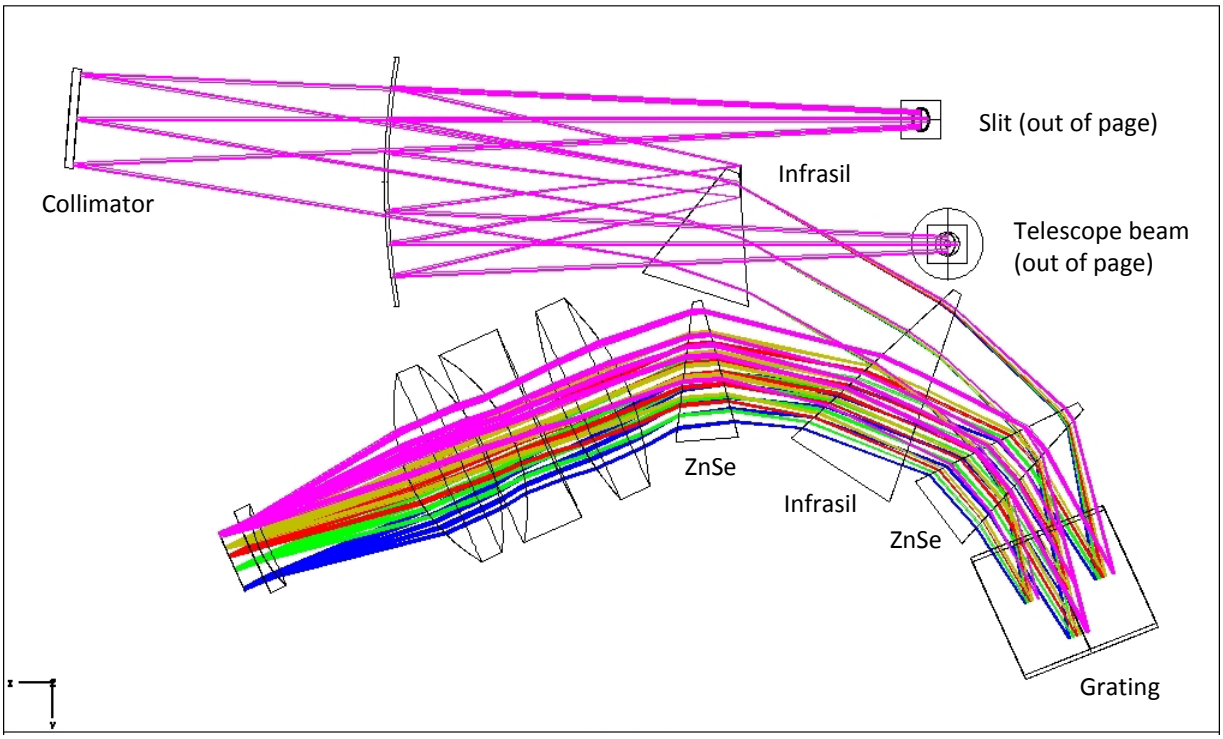

Figure 3: Optical layout of FIRE. The pre- and post-slit optics lie on separate planes above and below the page, so that the Offner relay is on the opposite side of the optical bench from the low background spectrograph.

The collimator is a single, off axis parabolic mirror and the refracting camera includes only 4 elements. Beam-folding mirrors are used for efficient packaging, and to isolate spatially the pre-slit portions of the instrument (which see full broadband sky) from the low-background, dispersed portion of the spectrograph. The entire optical train may be inscribed in a circle 75 cm in diameter.

The diameter of the collimated beam is 50 mm. This provides the desired wavelength resolution with an effective focal length of 180mm in the spectral direction while keeping the size and cost of the instrument within bounds. The design utilizes an R1 echelle grating (46° blaze angle) with 54.5 lines/mm, purchased from the Newport/Richardson Grating Lab. The grating is used in quasi-Littrow configuration over orders 11-32. The free spectral range and central wavelength of each order are diagrammed in Figure 5, which shows the echelle footprint on the detector. The optical configuration and detector area allow a 7 arcsecond long slit with sufficient order separation (> 1 arcsecond) on the detector at all wavelengths.

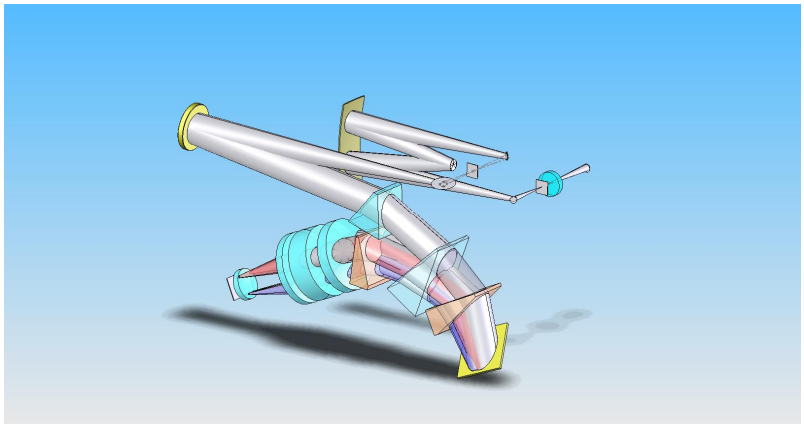
Figure 4: 3D rendering of the optical layout, emphasizing the different planes of the Offner relay and spectrograph optics.

In addition to its normal echellette mode, the spectrograph can be configured in a prism-only mode by swapping the echelle grating for a flat mirror. Because the prisms' materials and thicknesses have been have been optimized based on order spacing, the spectral resolution does not change monotonically; rather, it follows the spacing between the central wavelengths of the orders when the grating is in use. The resolution (in low-dispersion mode) at any wavelength also depends on the variable F/# with wavelength, which changes due to beam

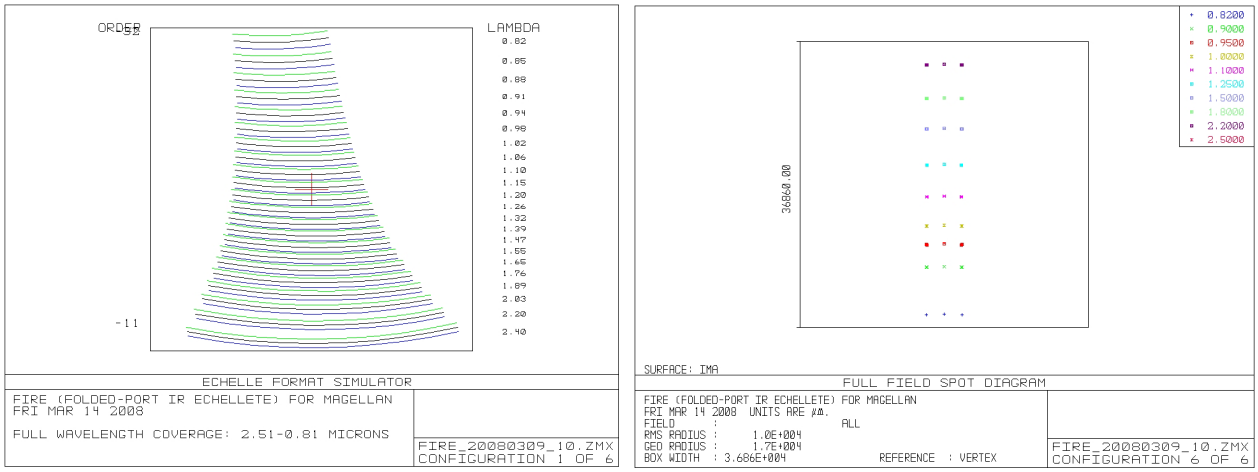

Figure 5: Spectral format at the detector for echellette mode (left) and low-dispersion longslit mode (right).

dilation through the prisms even when a mirror replaces the grating.

2.1 Fore-optics

In front of the slit, a 1:1 cold Offner[5] relay re-images the telescope pupil and provides a position for a cold stop. As in all IR spectrometers, up to [5,20]% of the light entering a [0.6,0.3] arcsecond slit is scattered out of the f/11 beam by diffraction effects; by placing the Offner before the slit, we prevent diffracted thermal emission from contributing to the diffuse background in the spectrometer. After the slit, the beam is bent in the plane of the page towards the f/11 collimator, which is a single, off-axis parabolic mirror. The image quality after the collimator is better than 0.1 arcsecond RMS as estimated using a paraxial (perfect) camera placed at the exit pupil of the collimator. Off-axis aberrations are concentrated in the spatial direction of the echellette slit, and are negligible across the seven arcsecond slit length. This permits use of a longer slit for low-dispersion mirror mode since for this orientation the beam is off-axis in the spectral direction. In low dispersion mode, the collimator delivers quality images over approximately a 1 arcminute field-of-view.

2.2 Prisms

FIRE employs a combination of two ZnSe and two fused silica prisms for cross-dispersion. These two materials are well matched to deliver uniform spacing between orders in the cross dispersion direction. Two of the four prisms (one apiece of Infrasil and ZnSe) are used in double-pass mode for a total of six passes. Besides reducing the total amount of glass, the use of double-pass construction controls the camera-collimator angle off of the diffraction grating, which in turn reduces the effects of anamorphic distortion from the prisms at the focal plane.

Careful attention was given to the optimization of prism tilts, apex angles, and materials. The goals of this optimization were to 1) space orders evenly across the full detector with adequate inter-order spacing for scattered light subtraction, 2) minimize variations in the spatial pixel scale arising from anamorphic distortions, 3) maintain sensible mechanical clearances for mounting hardware, 4) minimize thickness of ZnSe prisms, out of cost and material availability considerations, and 5) minimize the number of steep incidence angles at coated vacuum/glass interfaces.

The ultimate thicknesses of the ZnSe prisms are 43 and 36mm, compared to a maximum of 69mm for fused silica. The ZnSe prisms are being manufactured by II-VI infrared, and the used silica is Infrasil, grade 301 from Heraeus.

Figure 5 illustrates the resulting footprints at the detector in echelle and low-dispersion modes. For echelle mode, only the free spectral range of each order is shown to illustrate the fill pattern on the detector. Variations in the pixel scale are apparent in the figure; from the reddest to bluest orders the individual pixels range from 0.12 to 0.09 arcseconds

(compared to 0.18 in the spectral direction). In low-dispersion mode, the dispersion varies non-linearly, according to the tradeoff of ZnSe and Infrasil dispersion selected to achieve uniform order separation for the echelle.

2.3 Camera

The camera contains 4 refracting elements of materials CaF_2, S-FTM-16, CaF_2, and fused silica, respectively. The camera is optimized initially in the idealized situation of a well-defined entrance pupil and collimated beam; however the final optimization is performed with the complete optical system. This is critical because the optical axis of the beam that defines each field position in the focal plane is a result of the changing reflective and refractive angles off the grating and prisms and because the wavelengths sample different regions of the camera. The orientation of the collimated beam at each wavelength is important. As this suggests, the optimization is sensitive to the (gross) rotation angles of the prism and camera. The camera is fixed at an effective focal length of 180mm, which corresponds to a focal ratio of roughly 3.3 in the spectral direction at all wavelengths.

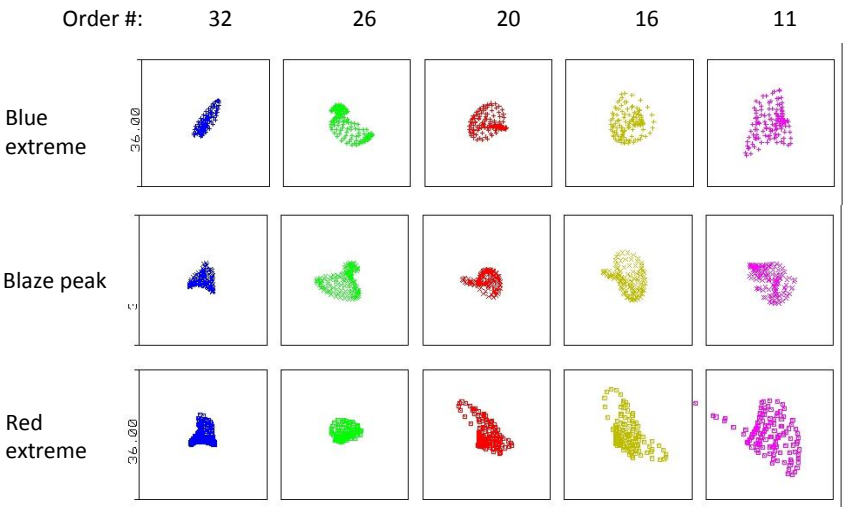

Figure 6: Spot diagrams across the echelle footprint. Boxes are 2 x 2 pixel regions 36 microns square. From right to left, various orders are shown from the bluest to reddest on the detector. From top to bottom, the blue, center, and red extremes of each order's free spectral range (FSR) is indicated. RMS spot radii are well within a single pixel over the full echelle format.

Spot diagrams are shown in Figure 6 for a range of orders on the detector. The spot matrix indicates the image quality as a function of wavelength and order number from the bluest order (#32 at 0.81 μm) to the reddest (order 11 at 2.5 μm). Naturally, the best images occur near the center of the detector, which maps to roughly 1.4μm.

An explicit effort was made to reduce the intensity of image ghosts and pupil ghosts where the initial bounce was from the detector surface. The most problematic ghosts originate between the detector and the field flattener. These have been reduced by forcing the field flattener back from the detector slightly and by forcing the surface of this negative element to be substantially concave away from the detector. As would be expected, the image quality is best when no location or figure constraints of this sort are placed on the elements during optimization, so the image quality is directly affected. The current compromise has image ghosts forming no closer than 50mm to the detector. At ~f/4, this implies ghost images diffused to roughly 12mm in diameter, or 1/3 of the detector. Pupil ghosts are no closer than 25 mm, or ~6 mm in diameter. Without constraining the ghosting at all during optimization, both image and pupil ghosts will form within 1 mm of the focal plane.

3. MECHANICAL STRUCTURE

FIRE is explicitly designed for operation at one of Magellan's auxiliary Nasmyth ("folded") foci, which are addressed by rotating the telescope tertiary to one of three ports between the altitude bearings. These ports have the advantage of continuous up-time and rapid access (~15 minutes for instrument changes during the night). But this comes at the expense of more limited access for servicing, significant weight restrictions, and varying gravity vector because of telescope pointing and field rotation about the bore sight.

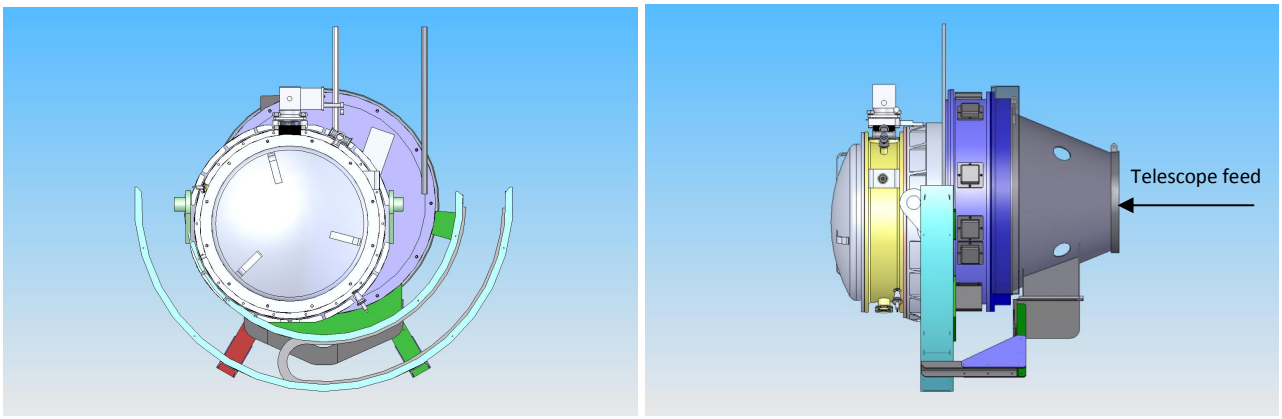

Figure 7: FIRE mechanical model, illustrating the orientation of the cryostat, instrument rotator, and cable wraps. Not shown are electronics racks, which mount to the rails visible at upper right.

Figure 7 shows front and side views of the main instrument assembly. The telescope beam enters from behind the page or to the right, in the left and right panels, respectively. In the right panel, the grey cone and dark blue assemblies are observatory-furnished guider/rotator packages. These units contain dual pickoff mirrors that are used for telescope guiding, and also Shack-Hartmann sensing to correct the telescope's primary mirror figure. The gusseted light grey and yellow dome shows the instrument cryostat, which maintains FIRE's optics and detector at a working temperature of 77K. Cooling is achieved via a single-stage, CTI 1050 closed cycle refrigerator, since access for LN2 feeds is limited at the folded ports. The refrigerator is mechanically isolated from the cryostat via a stage with very large lowest resonant mode, Sorbothane damping gaskets and a flexible bellows vacuum coupling. The dewar has a noticeably flat layout; this is because the plane of FIRE's optics has been folded into a vertical orientation, to keep assemblies close to the rotator and minimize flexure. The dewar has an outside diameter of 96 cm, and a total back distance of 80 cm from the telescope mounting surface.

FIRE's opto-mechanical assemblies reside on a 33 inch diameter optical bench, fabricated of 6061-T6 aluminum. Optics are mounted on both sides of this bench. The side facing the telescope houses the Offner relay, as well as a small slit-viewing camera that images reflected light onto an engineering-grade HAWAII-2RG focal plane array. Although telescope guiding is nominally controlled by optical pickoffs in front of the cryostat, the slit viewing optics are included to provide a native, infrared object acquisition system. After the slit, the beam entering the spectrograph is then folded through a small opening on the optical bench. The side facing away from the telescope houses the spectrograph opto-mechanics, described in Section 4.

Careful attention was given to the effects of flexure, and tolerance buildup during fabrication and assembly as they affect positioning of the optical bench. The bench itself is suspended in the cryostat via a quartet of G10 fiberglass tabs, which are in turn mounted to a very stiff Al ring. The support ring is a two sided flange that is decoupled from any chamber walls, so the mount points for the G10 will not flex when the dewar is evacuated. This ring is then indexed back to the telescope structure through a single stiff, gusseted riser that encompasses the back dome of the cryostat. Finite element analysis was employed in the dimensioning of the G10 supports, ring, and riser. The final design is expected to allow ~2mm shrinkage of the optical bench, while limiting flexure to 0.1 pixel or less at the focal plane, over an instrument rotation of 90 degrees. A significant uncertainty in the finite element analysis concerned the bulk and yield moduli of G10 at operating temperatures. To verify our design, we contracted for strain/yield testing of the actual G10 sheet purchased for the instrument, at 77K.

FIRE's slit-viewing camera provides a channel for compensating flexure that manifests as telescope pointing errors. Since the cold slit-viewing optics are mounted on the optical bench, they move together with the cold mass. Typical, rapid cadence guiding is controlled by the observatory's optical pickoff system (located outside of the dewar). The main function of the IR slit viewer is target acquisition, but it can also be run in long-exposure mode during spectroscopic

integrations, to monitor object drift on the slit from flexure of the cold mass relative to the rotator. Correction for these pointing errors will be servo relayed back to the telescope control system for closed-loop control.

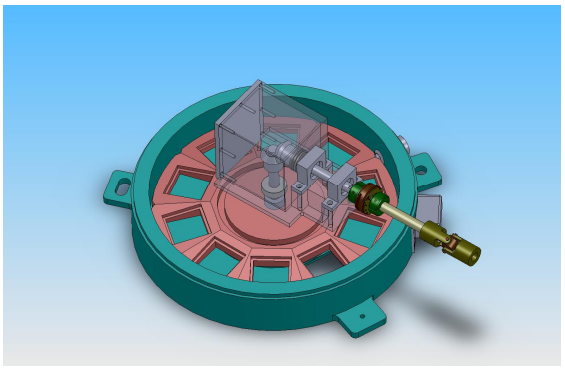

Figure 8: Mechanical model of the slit selector assembly, covers removed.

4. OPTO-MECHANICAL ASSEMBLIES

Like FIRE's optical bench, all cold opto-mechanical assemblies are constructed entirely from 6061-T6 aluminum, to mitigate stress from CTE mismatches at cool down. Where glass elements are present, we have employed customized kinematic mounts to minimally constrain each element and preload with customized springs. Final designs for most opto-mechanical subassemblies are now near convergence; these units will be certified through prototype testing in our lab's thermal vacuum test chamber before integration into the FIRE cryostat.

4.1 Slit selector

FIRE's entrance slits are being manufactured using precision electroforming techniques developed by Metrigraphics. This process yields slits with width variations at the micron level, or 0.5% for a 0.6 arcsecond slit. This precision is far better than typical mechanical fabrication or etching techniques, and is important for accurate flat fielding, illumination correction, and sky subtraction. FIRE's 1 x 1 inch slit plates will reflect a 50 arcsecond FOV back to the acquisition imager. The 10 individual plates are mounted on a detented 6 inch wheel, and driven by a stepper motor exterior to the dewar via a ferrofluidic vacuum feedthrough bearing. Since this assembly resides at the boundary between the imaging and spectroscopic sides of the instrument, keyed geometry was used at all interfaces to insure light-tight construction.

4.2 Collimator

FIRE's off-axis paraboloidal collimator is one of the two powered elements in the instrument whose position can be adjusted at cold operating temperature. A custom designed kinematic mirror cell holds the optic in place. This cell is in turn mounted on a twin-beam flexure stage that is compliant in the focus direction but extremely stiff in other directions. The stage was derived from a design used for alignment of fiber-optics in the telecommunications industry. It was specially prepared for vacuum cryogenic use by Luminos Industries.

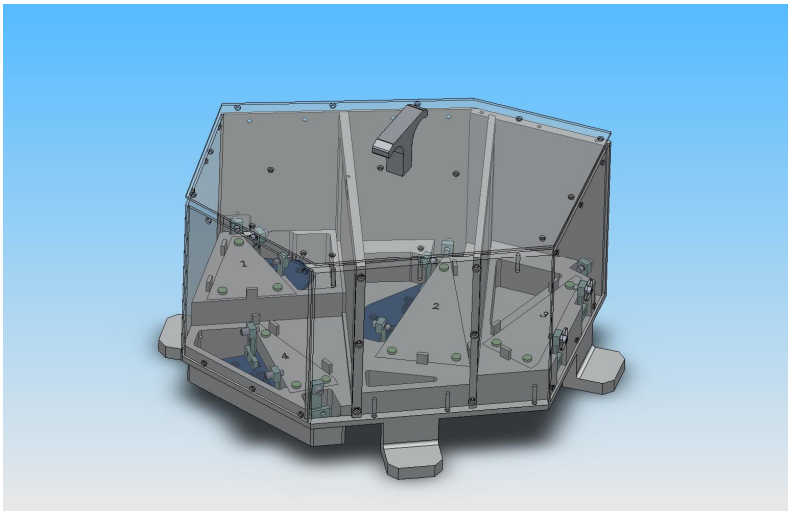

Figure 9: Cutaway of the prism mounting assembly, shown without prisms installed.

4.3 Prism assembly

FIRE's four prisms are located at the heart of the optical layout. They are mounted kinematically within a single, light-tight enclosure that is among the most complex sub-assemblies in the instrument (Figure 9). The optical performance of the spectrograph is only weakly sensitive to the detailed orientation and alignment of the prisms. Alignment requirements are comparable to machining and fabrication tolerances, so we elected to machine the defining points for all the prism mounts directly into a common block of aluminum. This block sets the relative heights and tilts of each prism, and is intended to reduce time and error associated with alignment of individual mounts at assembly phase. All hard stops are located in the bottom plate of the figure. Custom engineered leaf springs

terminated with threaded Teflon toggle pads provide precise, adjustable preloads and spring constants for each optic, in line with hard stops so as not to induce bending stress in the prisms.

The assembly's interior walls, and three extra internal baffles, are all painted with Aeroglaze Z306. These surfaces help to reduce stray light, and also provide a cold black surface for radiative coupling to the unpolished/uncoated sides of the prisms during cool down.

4.4 Grating/mirror turret

User selection of echellette versus low-dispersion mode is achieved by rotating the diffraction grating out of the beam and replacing it with a flat mirror. This binary mechanism is the most challenging moving part in the instrument because of weight and flexure concerns.

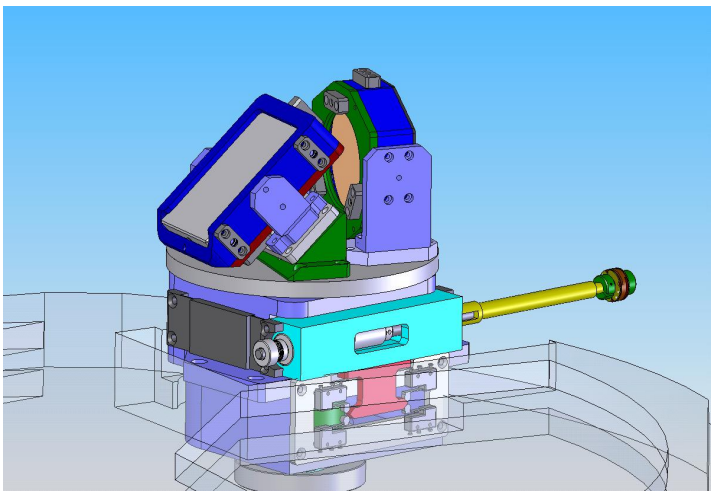

Figure 10: Grating/mirror turret solid model, illustrating worm shaft on flexure stage.

Our design is modeled after the grating turret in the MOSFIRE instrument for Keck, with slight modifications. Its single requirement is to deliver stiff, repeatable positioning in two different states. A stock aluminum bronze worm gear is oriented to drive the turret against clockwise and counter-clockwise hard stops. A floating bearing block consisting of the worm shaft, plus its bearings and axial retainers, is coupled to the main turret assembly by twin beam flexures. Thus when the hard stop is reached, the entire worm shaft block displaces with the flexures to load the turret against the stop. A doubly redundant set of limit switches prevents damage to the mechanism by accidental motor overrun.

Overall radial stiffness of the turret is achieved through use of cryogenically prepared thin-section bearings located near the spindle's center of mass. The axial load is compensated by spring washers that hold the spindle against the thin section bearing.

4.5 Detector stage

The science detector will be mounted on a Molybdenum stage that is thermally isolated from the rest of the instrument via a G10 A-frame structure. The temperature of this stage is controlled using an external Lakeshore controller. Because the detector receives a fast beam from the camera and is therefore sensitive to focus, we chose it as a location for a cold-adjustable focus. Cryogenic motion is achieved by mounting the detector A-frame to an identical structure as the collimator: an all-aluminum twin beam flexure from Luminos industries. The camera's field flattener is mounted to this stage and moves with the detector during focus.

5. DETECTORS

FIRE employs two HAWAII-2RG focal plane arrays (FPAs), from Teledyne Scientific & Imaging. One of these arrays is a science grade device to be used in the low background, spectrograph channel of the instrument. The other FPA is an engineering grade device, and will be used for the slit viewing imager channel. For the slit viewer, we will only use a 512 x 512 square region of the detector (because of the Offner relay's limited FOV) and noise requirements are less stringent than for the spectrograph detector.

Both detectors are read out using Teledyne's SIDECAR ASIC circuitry, which we plan to install in the cryogenic environment. The decision to use the SIDECAR was motivated in part from a desire to maintain a single IR readout architecture for the observatory – another major instrument (the FourStar mosaic imager) will be delivered to Magellan

on similar timescales, and it makes heavy use of SIDECAR electronics. FIRE's readout software is being developed in close communication with the FourStar team, to insure compatibility where appropriate.

The SIDECAR units, together with cryogenic circuit boards for ground-based development, were delivered in early 2008 and are currently undergoing warm testing. The boards have completed warm performance verification after multiple cold cycles, but actual cold performance verification is still pending. Testing of our science and engineering grade detectors will be completed using both the SIDECAR, and an independent set of well-characterized electronics in the University of Rochester lab. This procedure both certifies the performance of the HAWAII-2RG arrays, and isolates the effects of the SIDECAR on the signal chain.

6. SOFTWARE ARCHITECTURE AND DEVELOPMENT

6.1 Instrument control and data flow

FIRE's computing environment encompasses three networked nodes, at the instrument itself, the telescope computing room, and the user workstation. At the instrument, a pair of Windows-based PCs controls the SIDECARs and detector arrays. These machines contain minimal storage, and instead act as data buffers for transfer of images to the control computers in the computing center. The rest of the network is Macintosh-based, following Magellan observatory convention. The Mac machines in the computing room provide space for data storage, send commands to temperature and motor controllers over Ethernet/serial links, and receive feedback from the same. Users in the control room log into these computers via VPN and execute control commands remotely.

Our general instrument control and monitoring software is derived from code already implemented at Magellan; we have purchased compatible hardware to make FIRE's integration with this existing system as transparent as possible. However, we are developing a separate user interface for initial viewing and rudimentary analysis of incoming data. This system is built on a port of the DV image viewing library (maintained by the IRTF) to the Macintosh environment. Separate DV windows will be used to monitor FIRE's spectroscopic and imaging channels. We are including slight modifications to the standard DV package to support some of the guiding functionality that is built into FIRE's slit viewing channel.

6.2 End-user software

Since FIRE is being constructed with facility instrument status in mind, our team is providing observers with software tools for data reduction. We will provide a suite of open-source IDL utilities for reduction and calibration of point-source data. This software will be developed by modifying and extending existing pipelines for other instruments that are familiar to our team.

FIRE's data flow will have a similar look-and-feel to the SpeXtool[7] reduction package supported by the IRTF. GUI based widgets sit above an optional command line interface that is provided for more advanced users. The GUI applications will be evolved directly from the available code base for SpeXtool.

However, the underlying code for wavelength mapping, sky subtraction, and extraction will employ additional techniques developed for other instrument pipelines, including GNIRS (written by Simcoe), MIKE (by S. Burles, J. Prochaska, and R. Bernstein), and MagE (Simcoe and J. Hennawi). These methods are loosely based on the Poisson-limited sky subtraction algorithm described by Kelson et al[8], which takes advantage of the "tilt" of the slit relative to detector pixels, to obtain a sub-sampled model of the sky in slit pixels not contaminated with object flux. Traditional A/B pairwise sky subtraction will also be supported for completeness. However, for the faint objects we intend to target with FIRE, an effective model of the sky for each individual frame should reduce noise introduced by pairwise subtraction, and could also open the possibility for longer individual integration times.

In addition to the full reduction package, we will release a quick-look package and a FIRE simulator, to aid in quality assurance at the telescope and planning of observations. The FIRE simulator software is already complete, having grown out of efforts to estimate instrument throughput during design. The software is capable of simulating 1D

extracted spectra, or 2D spectral images, and will be used to test the reduction software until the instrument is functioning. Upon commissioning, we will simply replace our theoretical estimates of throughput with zero points obtained from standard stars. The quick-look reduction pipeline will essentially mimic the full reduction suite, except that it will use archived wavelength, flat field, and sensitivity functions, and perform boxcar extraction only.

ACKNOWLEGEMENTS

It is a pleasure to thank the many people who have lent their time, expertise, and support to the FIRE project. In particular, we acknowledge the contributions of Ian McLean, John Rayner, Stephen Smee, John Wilson, Eric Persson, Steve Shectman, Alan Uomoto, Christoph Birk, Jen Marshall, Mike Skrutskie, Bob Weber, Frank Perez, Neil Pappalardo, Curt Marble, and the MIT Physics department. FIRE's construction is supported by the National Science Foundation under the MRI program, grant number AST-0619490.

REFERENCES

[1] Martini, P. and DePoy, D., 2000, Proc. SPIE Vol. 4008, p. 695-702
[2] Rousselot, P., Lidman, C., Cuby, J.-G., Moreels, G., and Monnet, G., 2000, Astronomy & Astrophysics, 354, 1134
[3] Maihara, T. et al, 1993, PASP 105, 940
[4] Ellis, S. & Bland-Hawthorn, J., 2008, MNRAS, 386, 47
[5] Sheinis, A. et al, 2002, PASP, 114, 851
[6] Offner, A., 1970, in *Optical Telescope Technologies*, p. 321
[7] Cushing, M., Vacca, W., & Rayner, J. 2004, PASP 116, 362
[8] Kelson, D, 2003, PASP 115, 688